Synthesis and characterization of TiO$_2$@C core-shell nanowires and nanowalls via chemical vapor deposition for potential large-scale production

Hao Liu [a], Yong Zhang [a], Ruying Li [a], Mei Cai [b], Xueliang Sun [a,*]

[a] Department of Mechanical and Materials Engineering, The University of Western Ontario, London, ON, Canada N6A 5B9
[b] General Motors Research and Development Center, Warren, MI 48090-9055, USA

ARTICLE INFO

ABSTRACT

TiO$_2$ nanowires and nanowalls core structures covered with carbon shell were selectively synthesized by a simple chemical vapor deposition (CVD) method using commercial titanium powder as the starting material. Morphology and structure of the products were characterized by scanning electron microscopy (SEM) and transmission electron microscopy (TEM). The core shell structure is composed of single crystalline rutile titanium dioxide wrapped by amorphous carbon shell. By adjusting the growth temperature, morphology of the products can be controlled from one-dimensional nanowires to two-dimensional nanowalls. While TiO$_2$@C nanowires were a preferred structure at higher temperature, TiO$_2$@C nanowalls dominated the final product at lower temperature. A growth mechanism was proposed based on the initial growth state of these nanostructures, in which solid-state diffusion of the elements involved in the reaction was assumed to play an essential role. The obtained TiO$_2$@C core shell structures may find potential applications in various nanoscale realms such as optoelectronic, electronic and electrochemical nanodevices and the simple synthesis procedure promises large scale production and commercialization of the titanium oxide@carbon nanostructures.

1. Introduction

With a wide band gap of 3.2 eV, titanium dioxide is an n-type semiconductor material, possessing superior photo electrochemical conversion properties, excellent chemical and thermal stability, good electrical and optical properties, which make it suitable candidates for solar cells [1,2], photo-degradation [3] and photocatalysis [4], optical [5–7] and electronic [8,9] devices, gas sensors [10,11], waste water purification and self-cleaning coatings [12,13]. With the research marching into nanoscale regime, anisotropic TiO$_2$ nanostructures, such as nanofilms [1], nanorods [14], nanowires [15], nanowalls and nanotubes [16] have stimulated great interest due to their large specific surface area, high sensitivity and activity, which significantly enhanced the applications based on their properties. However, improving the photocatalytic efficiency of TiO$_2$ to meet the practical application requirement is still very challenging, mostly due to the low yield caused by the rapid recombination of photogenerated electrons and holes [17]. One method to increase the electron–hole separation efficiency is to form a heterostructures which could provide a potential driving force for the separation of photogenerated charge carriers [18]. It has been reported that carbon nanotubes (CNTs) could increase the photocatalytic activity of TiO$_2$ because the excited electron in

conducting band of TiO$_2$ might migrate into the CNTs and prevent the recombination of electron–hole pairs [19].

Carbon nanostructures have attracted great interest because of their chemical compatibility, as well as the superior mechanical, thermic and electronic properties compare to the conventional bulk carbon materials. CNTs have tremendous potential for applications in electron field emitter of displays [20,21], nanoscale electronic devices [22], biosensors [23], hydrogen storage [24] and fuel cell electrodes [25]. Carbon nanowalls also have unique field-emission and electron transport properties. Free-standing and vertically oriented surface morphology of the carbon nanowalls carries a large surface-to-volume ratio, which makes it an ideal functional support for synthesizing composite material with large surface area. Until now, approaches have been made to use carbon nanowalls as catalyst support with magnetic nanoparticles [26] and platinum [27] coated on surface by electrodeposition.

With respect to the potential of titanium oxide and carbon nanostructures on catalysis fields, the composition of these two kinds of structures may promise a novel hybrid structure with synergetic functional effect compared to the two individual structures. Recently, TiO$_2$@C core shell particles have been synthesized, and their great potential on photocatalysis and electrocatalysis have also been addressed [28,29]. However, to our best knowledge, one-dimensional or two-dimensional TiO$_2$@C has rarely been reported. In this study, we synthesized TiO$_2$ nanowires and nanowalls covered by amorphous carbon from Ti powder. Due to the high

* Corresponding author. Fax: +1 519 661 3020.
E-mail address: xsun@eng.uwo.ca (X. Sun).

melting point of titanium and relatively low vapor pressure of the titanium powder at the temperature used in this work, we propose a new growth mechanism based on the diffusion of titanium and oxygen ions.

2. Experiment

The titanium powder (100 mg) was put in an Al_2O_3 boat which was placed in a quartz tube. The whole system was then placed in a simple horizontal quartz tube furnace, in which the oxidation of the Ti powder was carried out. Pure argon (99.999%) was first introduced to the system at a flow rate of 400 sccm for about 2 h to flush out the air in the tube. The furnace was then heated with a heating rate of 60 °C/min until the temperature reached target temperatures from 850 °C to 950 °C. Meanwhile the argon flow rate was reduced to 5 sccm and acetone was introduced into the reaction chamber through a water bubbler containing 5 vol.% acetone in water using argon as carrier gas. The temperature was maintained at the target temperature for 2 h before cooling down to room temperature under the same atmosphere.

The samples were characterized by Hitachi S-4500 field-emission scanning electron microscope (SEM) operated at 5.0 kV, Philips CM10 transmission electron microscope (TEM) operated at 80 kV, and a JEOL 2010 FEG transmission electron microscope (TEM) at 200 kV for high-resolution imaging and selected area electron diffraction (SAED) determination.

3. Result and discussion

Fig. 1 shows the general morphology of TiO_2 nanostructures grown on the titanium powder using this simple CVD method. Fig. 1a–c are taken from the samples synthesized at 850 °C, 900 °C and 950 °C for 2 h, respectively. Uniform nanostructures were observed in all these SEM images. Since the titanium powder was used as both the starting material and the substrate, the product morphology shows ball-like feature. With the reaction duration, the titanium core can be gradually oxidized. At the temperature of 850 °C shown in Fig. 1a, the representative structures observed on the surface of original TiO_2 were nanowalls with a width around 150 nm. The nanowalls had an orientated growth direction perpendicular to the surface of the particles. Other than nanowalls, some nanorods were also observed from the side view of the nanostructure at the low right corner in Fig. 1a. At a higher temperature of 900 °C, shown in Fig. 1b, much more nanorods were found on the surface of the powder besides the nanowalls. The difference can be seen clearly from the side view of the sample at low right corner in Fig. 1b. When the temperature reached 950 °C shown in Fig. 1c, almost all the surface of the particles was covered with nanorods, with a diameter of less than 200 nm; meanwhile the length of the nanowalls became smaller than that of the ones synthesized at lower temperature. When the temperature was continuously increased, the morphology of nanowalls and nanorods disappeared and the surface of the particle was totally oxidized into dense polycrystalline grains which are not shown here. When the temperature was lowered to 800 °C, neither nanowalls nor nanorods were observed. Among all the concentrations we have tried from pure water to pure acetone under this argon flow rate, it appears that 5% acetone in water is the best concentration for the growth of nanostructures. Meanwhile, different argon flow rates have also been studied. The results show that as the increase of argon flow rate, more carbon would be brought into our reaction, and the starting titanium powder will be covered by a thick layer of carbon and no nanostructures can be observed from the titanium powder and when the argon flow rate decreases, oxygen is not sufficient in the reaction and a slow oxidation hap-
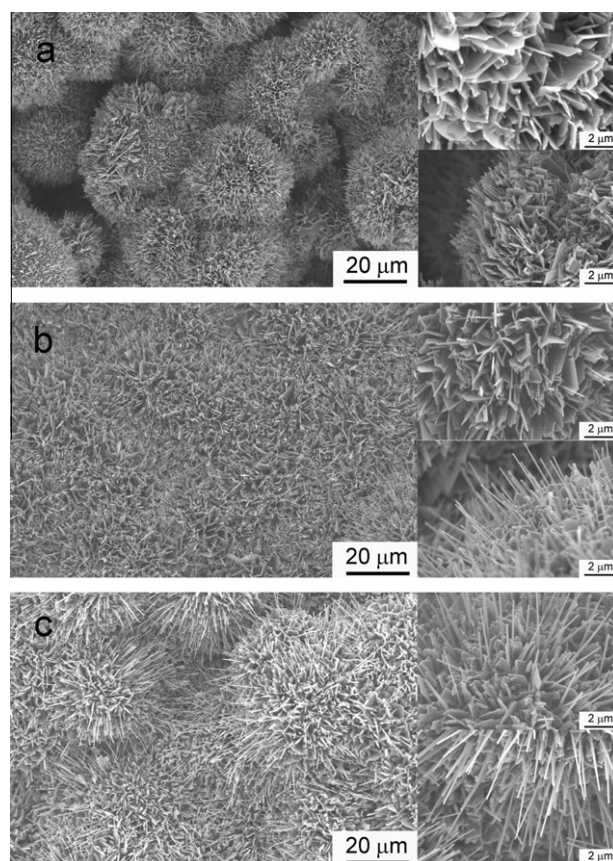
Fig. 1. SEM images of $TiO_x@C$ nanostructure grown at (a) 850 °C, (b) 900 °C and (c) 950 °C for 2 h respectively on titanium powder without catalyst. The picture at the up-right corner is a high magnification top-view image and the picture at the down-right corner is a high magnification side-view image.

pens and no nanostructure can be observed, either. Our systematical study show that the best condition for the growth of carbon covered TiO_2 nanowires is 950 °C at 5 sccm of argon through a water bubbler containing 5 vol.% acetone in water. The best condition for the growth of carbon covered TiO_2 nanowires is almost the same unless the temperature is lowered to 850 °C.

Further characterization of the structure was carried out by using transmission electron microscopy (TEM). The TEM images of a typical nanorod and nanowall are shown in Fig. 2a and b, separately. A relatively lighter color is observed on the side of both nanorod and nanowall. Energy dispersive X-ray spectrometry (EDX) analysis detected that the light part is carbon and energy filtering TEM (EFTEM) mapping reveals that these TiO_x nanostructure are all covered by a layer of carbon. It can be seen that the diameter of the carbon covered nanowire is less than 100 nm while the width of the nanowall can reach 1 μm.

High resolution TEM (HRTEM) image in Fig. 3 shows that both nanowalls and nanowires are single crystal with an inter-planer spacing of 0.248 nm, in agreement with the d value of the (101) planes of the tetragonal rutile TiO_2 crystal structure whose lattice constants are $a = 4.593$ Å, $c = 2.959$ Å and the space group is $P4_2/mnm$ (136) [JCPDS 21-1276]. The corresponding selected area electron diffraction (SAED) was recorded in the image inserted in Fig. 3, the bright diffraction spots indicate single crystalline structure of the nanowires. The lattice fringes of (101) crystal planes in the nanowire are perpendicular to the longitudinal axis of the nanowire, revealing that [101] is the favored direction of growth of this TiO_2 nanowires. This indicates faster growth rate along the [101] direction than other crystal directions, resulting in
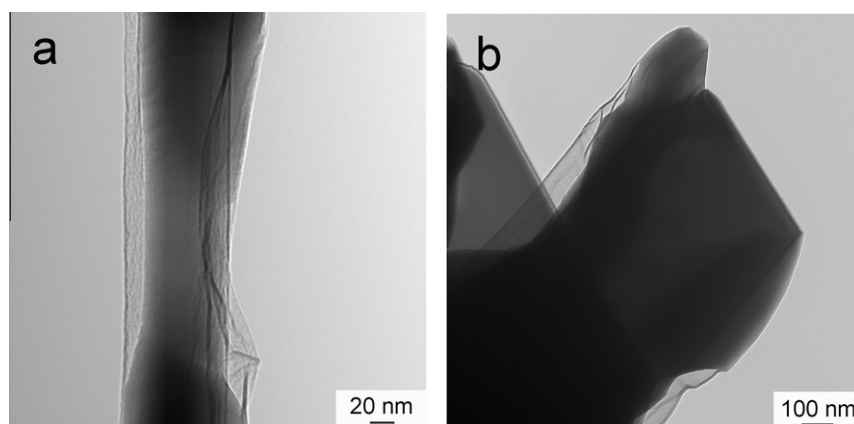
Fig. 2. TEM images of TiO$_2$@C nanostructures: (a) nanorod and (b) nanowall.
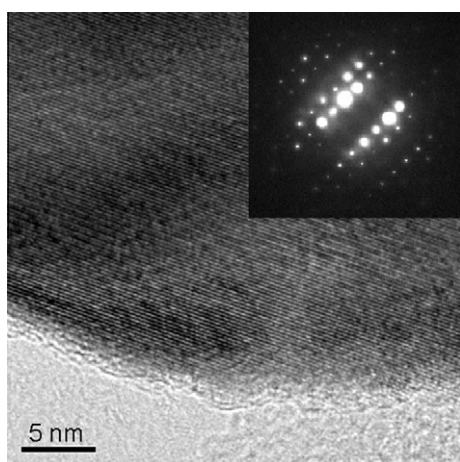
Fig. 3. HRTEM image and related selected area diffraction pattern of the synthesized structure.

one-dimensional nanowires. The SAED patterns for both kinds of nanostructures are the same.

4. Growth mechanism

The formation mechanism of the TiO$_2$ nanowires is different from that of the vapor–liquid–solid (VLS) mechanism because it is a catalyst free process and that of vapor–solid (VS) model due to high melting point of metal titanium (1660 °C). To understand how the carbon-covered TiO$_2$ nanostructures are formed, a series of experiments at 850 °C using different heating duration were employed to study the initial state of the growth of nanowalls and nanowires. Fig. 4 shows the SEM images of the nanostructures, with heating duration of 30 min, 60 min, 90 min and 120 min, shown in Fig. 4a–d, respectively. Fig. 4a reveals that TiO$_2$ seeds were formed as nanoclusters with a high surface energy at the first step of the process. With the growth time, Fig. 4b and c presents that some of the nanoclusters grew together forming the nanowalls while the remaining nanoclusters grew longer to form nanowires.
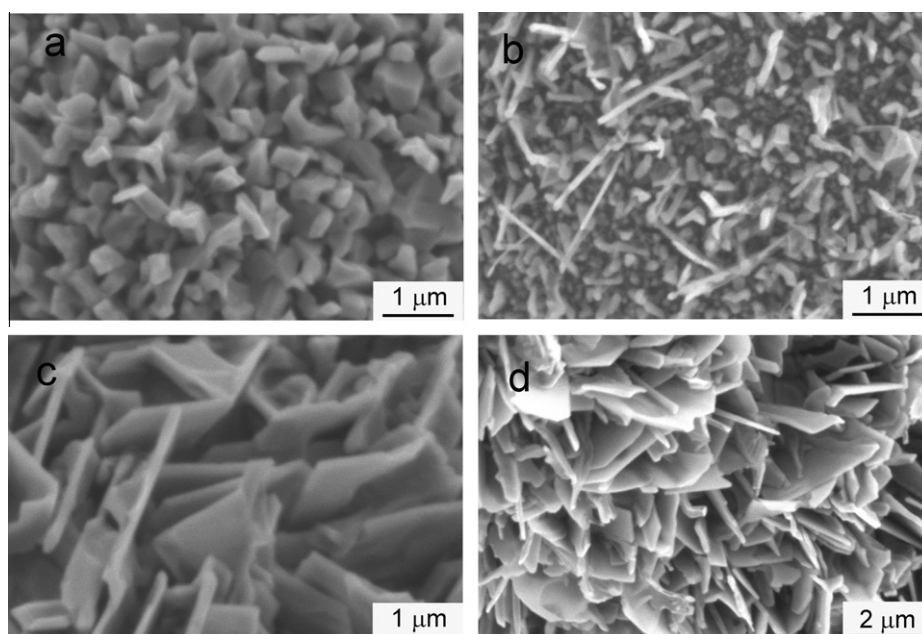
Fig. 4. SEM images of TiO$_x$@C nanostructures grown at 850 °C using (a) 30 min, (b) 60 min, (c) 90 min and (d) 120 min, separately.
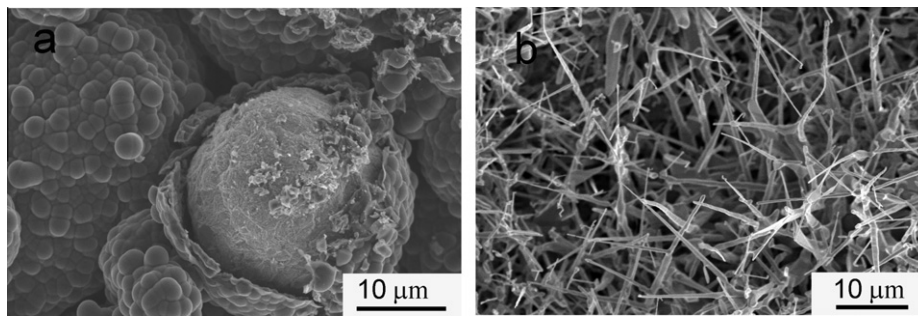
Fig. 5. SEM images of sample synthesized with (a) pure acetone and (b) pure water.

To help understanding the growth mechanism, experiments with pure water and acetone have also been carried out. SEM images of above experiments are shown in Fig. 5. With pure acetone, as shown in Fig. 5a, due to existence of big amount of carbon, carbon layer totally covered the surface of titanium particles. Meanwhile, nanowire structure with low density and non-uniform size was observed by using pure water.

Based on the above observation, a schematic mechanism is proposed and illustrated in Fig. 6 and we attribute the growth mechanism of this nanostructure to a solid-state diffusion process.

Initially, shown in Fig. 6a and b the surface of the Ti powder was oxidized by oxidative water vapor. Due to the existence of reductive carbon mono-oxide, which is decomposed from acetone [30], the reduction happened at the same time. Oxygen is partially removed from the TiO_2 surface to leave TiO_{2-x}, demonstrated in Fig. 6c. The resultant Ti interstitials such as Ti cations will rapidly diffuse from the surface into the bulk [31], as illustrated in Fig. 6d. The grain-boundary diffusion dominates the diffusion process over lattice diffusion [32] making the Ti cations accumulate in the grain boundaries, presented in Fig. 6e. As the accumulation proceeds to
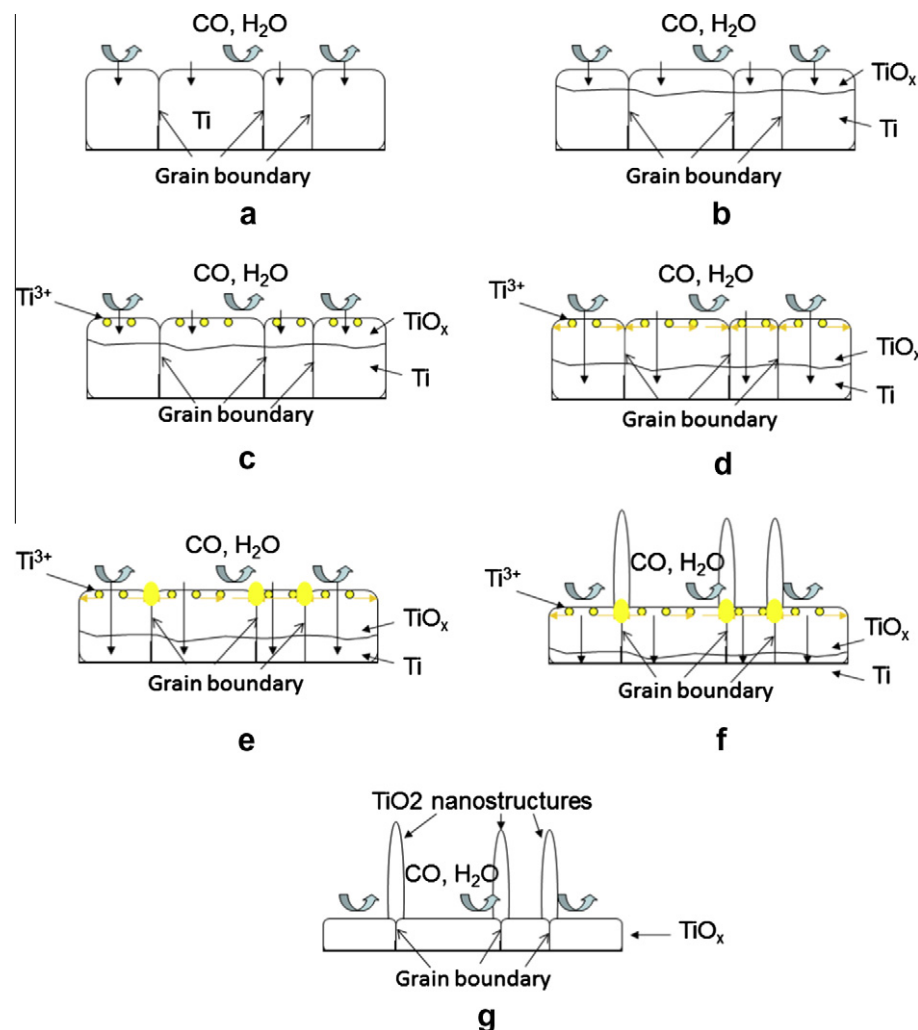
Fig. 6. Schematic illustration of the growth steps of carbon covered TiO_2 nanostructures. Black arrows are showing the diffusion direction of oxygen atom and yellow arrows are showing the diffusion direction of Ti cations. (For interpretation of the references to color in this figure legend, the reader is referred to the web version of this article.)

certain extend, the Ti cations are re-oxidized by the oxidative water vapor, exhibited in Fig. 6f. As the reduction, diffusion and re-oxidation proceed, nanowall structures are formed at grain boundaries and nanowires structures are arisen at the conjunctions of three grain boundaries, as shown in Fig. 6g. At higher temperature (950 °C), the diffusion of Ti cations is enhanced, then more Ti cations could diffuse to the conjunctions of three grain boundaries, then TiO_2 nanowires are preferred to be synthesized at high temperature. At lower temperature (850 °C), the motion of Ti cations decreases. Then most of Ti cations are accumulated at the grain boundaries giving rise to the dominance of nanowalls. When the temperature further decreases, no sufficient Ti cations could diffuse to the boundaries, and no nanostructures could be observed. On the other hand, simultaneous to the above process, carbon decomposed from acetone forms carbon layers on the surface of TiO_2. The presence of carbon atoms preferred to cover the surface of the TiO_2 where the growth is relatively slow while the crystallographic plane with higher growth rate cannot be covered. Then the nanostructures were driven to grow along a certain crystallographic orientation. This growth mechanism also explains the reason why the growth of TiO_2 did not begin soon after the target temperature was reached. The nucleation of the nanowires needs a longer time compared with the VLS growth mechanism. The reason why nanowire-like structures were also obtained using pure water, however, featuring low density and non-uniform size, is probably due to the weak reductive atmosphere generated by water vapor decomposition on the titanium oxide surface under high temperature.

5. Conclusion

TiO_2@C core shell nanowires and nanowalls were synthesized by a simple CVD method with a controllable structure by modulating experimental conditions. SEM, HRTEM along with SAED techniques were employed to investigate morphology and structure of these nanostructures. The proposed growth mechanism based on the solid-state diffusion was supported by the time dependent observation of the initial state of these nanostructures. The obtained single crystal TiO_2@C nanowires and nanowalls are expected to be a good candidate for the development and design of various optoelectronic, electronic and electrochemical nanodevices. And the simple synthesis procedures promise large scale production and commercialization of the core shell titanium oxide@carbon nanostructures.

Acknowledgments

References

[1] B. O'Regan, M. Grätzel, Nature 353 (1991) 737.
[2] T. Stergiopoulos, I.M. Arabatzis, G. Katsaros, P. Falaras, Nano Lett. 2 (2002) 1259.
[3] S.A. O'Neill, I.P. Parkin, R.J.H. Clark, A. Mills, N. Elliott, J. Mater. Chem. 13 (2003) 56.
[4] Y.-M. Sung, J.-K. Lee, W.-S. Chae, Cryst. Growth Des. 6 (2006) 805.
[5] J.E.G.J. Wijnhoven, W.L. Vos, Science 281 (1998) 802.
[6] A. Richel, N.P. Johnson, D.W. McComb, Appl. Phys. Lett. 76 (2000) 1816.
[7] D. Appell, Nature 419 (2002) 553.
[8] Y. Masumoto, M. Murakami, T. Shono, T. Hasegawa, T. Fukumura, M. Kawasaki, P. Ahmet, T. Chikyow, S. Koshihara, H. Koinuma, Science 291 (2001) 854.
[9] S.A. Chambers, S. Thevuthasan, R.F.C. Farrow, R.F. Marks, J.U. Thiele, L. Folks, M.G. Samant, A.J. Kellock, N. Ruzychi, D.L. Ederer, U. Diebold, Appl. Phys. Lett. 79 (2001) 3467.
[10] O.K. Varghese, D. Gong, M. Paulose, K.G. Ong, C. Dickey, C.A. Grimes, Adv. Mater. 15 (2003) 624.
[11] A. Rothschild, A. Levakov, Y. Shapira, N. Ashkenasy, Y. Komem, Surf. Sci. 532 (2005) 456.
[12] U. Diebold, Surf. Sci. Rep. 48 (2003) 53.
[13] P. Bonhote, E. Gogniat, M. Graztel, P.V. Ashrit, Thin Solid Films 350 (1999) 269.
[14] X. Peng, A. Chen, J. Mater. Chem. 14 (2004) 2542.
[15] B. Xiang, Y. Zhang, Z. Wang, X.H. Luo, Y.W. Zhu, H.Z. Zhang, D.P. Yu, J. Phys. D38 (2005) 1152.
[16] S.M. Liu, L.M. Gan, L.H. Lu, W.D. Zhang, H.C. Zeng, Chem. Mater. 14 (2002) 1391.
[17] W. Choi, A. Termin, M.R. Hoffmann, J. Phys. Chem. 98 (1994) 13669.
[18] H. Wang, X. Quan, H. Yu, S. Chen, Carbon 46 (2008) 1126.
[19] Y. Yu, J.C. Yu, J.G. Yu, Y.C. Kwok, Y.K. Che, J.C. Zhao, L. Ding, W.K. Ge, P.K. Wong, Appl. Catal. A. Gen. 289 (2005) 186.
[20] S. Fan, M.G. Chapline, N.R. Franklin, T.W. Tombler, A.M. Cassell, H. Dai, Science 283 (1999) 512.
[21] N. de Jonge, Y. Lamy, K. Schoots, T.H. Oosterkamp, Nature 420 (2002) 393.
[22] A.M. Fennimore, T.D. Yuzvinsky, W. Han, M.S. Fuhrer, J. Cumings, A. Zettl, Nature 424 (2003) 408.
[23] W. Huang, S. Taylor, K. Fu, Y. Lin, D. Zhang, T.W. Hanks, A.M. Rao, Y.P. Sun, Nano Lett. 2 (2002) 311.
[24] C. Liu, Y.Y. Fan, M. Liu, H.T. Cong, H.M. Cheng, M.S. Dresselhaus, Science 286 (1999) 1127.
[25] D. Villers, S.H. Sun, A.M. Serventi, J.P. Dodelet, S. Desilets, J. Phys. Chem. B 110 (2006) 25916.
[26] B. Yang, Y. Wu, B. Zong, Z. Shen, Nano Lett. 2 (2002) 751.
[27] L. Giorgi, Th.D. Makris, R. Giorgi, N. Lisi, E. Salernitano, Sens. Actuator B: Chem. 126 (2007) 144.
[28] S. Shanmugm, A. Gedanken, Small 3 (2007) 1189.
[29] S. Shanmugam, A. Gabashvili, D.S. Jacob, J.C. Yu, A. Gedanken, Chem. Mater. 18 (2006) 2275.
[30] J.R.E. Smith, D. Phil, C.N. Hinshelwood, Proceedings of the Royal Society of London, Mathematical and Physical Sciences A 183 (1944) 33.
[31] M.A. Henderson, Surf. Sci. 419 (1999) 174.
[32] S. Yoo, S.A. Dregia, S.A. Akbar, H. Rick, K.H. Sandhage, J. Mater. Res. 21 (2006) 1822.